

High sensitive chiral molecule detector based on the amplified lateral shift in Kretschmann configuration involving chiral TDBCs

Song Wang(王松), Qihui Ye(叶起惠), Xudong Chen(陈绪栋), Yanzhu Hu(胡燕祝), and Gang Song(宋钢)
Citation: Chin. Phys. B, 2021, 30 (**6**): 067301. DOI: 10.1088/1674-1056/abdda6
Journal homepage: http://cpb.iphy.ac.cn; http://iopscience.iop.org/cpb

What follows is a list of articles you may be interested in

Multiple Fano resonances in metal-insulator-metal waveguide with umbrella resonator coupled with metal baffle for refractive index sensing

Yun-Ping Qi(祁云平), Li-Yuan Wang(王力源), Yu Zhang(张宇), Ting Zhang(张婷), Bao-He Zhang(张宝和), Xiang-Yu Deng(邓翔宇), Xiang-Xian Wang(王向贤)
Chin. Phys. B, 2020, 29 (**6**): 067303. DOI: 10.1088/1674-1056/ab888c

Optical spin-to-orbital angular momentum conversion instructured optical fields

Yang Zhao(赵阳), Cheng-Xi Yang(阳成熙), Jia-Xi Zhu(朱家玺), Feng Lin(林峰), Zhe-Yu Fang(方哲宇), Xing Zhu(朱星)
Chin. Phys. B, 2020, 29 (**6**): 067301. DOI: 10.1088/1674-1056/ab862a

Coupling-induced spectral splitting for plasmonic sensing with ultra-high figure of merit

Hua Lu(陆华), Yi-Cun Fan(范奕村), Si-Qing Dai(戴思清), Dong Mao(毛东), Fa-Jun Xiao(肖发俊), Peng Li(李鹏), Jian-Lin Zhao(赵建林)
Chin. Phys. B, 2018, 27 (**11**): 117302. DOI: 10.1088/1674-1056/27/11/117302

Gap plasmon-enhanced photoluminescence of monolayer MoS_2 in hybrid nanostructure

Le Yu(余乐), Di Liu(刘頔), Xiao-Zhuo Qi(祁晓卓), Xiao Xiong(熊霄), Lan-Tian Feng(冯兰天), Ming Li(李明), Guo-Ping Guo(郭国平), Guang-Can Guo(郭光灿), Xi-Feng Ren(任希锋)
Chin. Phys. B, 2018, 27 (**4**): 047302. DOI: 10.1088/1674-1056/27/4/047302

Thermal emission properties of one-dimensional grating with different parameters

Weixin Lin(林伟新), Guozhou Li(李国洲), Qiang Li(李强), Hongjin Hu(胡宏锦), Fang Han(韩防), Fanwei Zhang(张樊伟), Lijun Wu(吴立军)
Chin. Phys. B, 2017, 26 (**5**): 057301. DOI: 10.1088/1674-1056/26/5/057301

High sensitive chiral molecule detector based on the amplified lateral shift in Kretschmann configuration involving chiral TDBCs*

Song Wang(王松)[1], Qihui Ye(叶起惠)[2,3], Xudong Chen(陈绪栋)[2], Yanzhu Hu(胡燕祝)[1], and Gang Song(宋钢)[2,†]

[1] School of Modern Post, Beijing University of Posts and Telecommunications, Beijing 100876, China
[2] School of Science, Beijing University of Posts and Telecommunications, Beijing 100876, China
[3] International School, Beijing University of Posts and Telecommunications, Beijing 100876, China

(Received 6 December 2020; revised manuscript received 2 January 2021; accepted manuscript online 20 January 2021)

We investigate a high sensitive chiral molecule detector based on Goos–Hanchen shift (S) in Kretschmann configuration involving chiral tri (diethylene glycol monobutyl) citrates (TDBCs). Fresnel equations and the stationary phase method are employed to calculate S. Due to the interaction between surface plasmon polaritons and chiral TDBCs, S with chiral TDBCs are amplified at near the resonant wavelengths of chiral TDBCs. Our calculation results show that although the difference between the resonant wavelengths of left and right TDBCs is 4.5 nm, the positions of the largest S for the structures with left TDBCs and right TDBCs do not overlap. S reaches 400 times (or 200 times) the incident wavelength around the resonant wavelength of left TDBCs (or right TDBCs). The difference of S with chiral TDBCs (ΔS) can reach 400 times or 200 times the incident wavelength in certain conditions, which can be directly observed in experiments. Left TDBCs and right TDBCs are easily distinguished. There is an optimal thickness of the metal film to realize the largest difference of S between Kretschmann configurations with left TDBCs and right TDBCs. Furthermore, we discuss the oscillator strength f, which is mainly determined by TDBC concentration. We find that our proposed detector is quite sensitive with f. By changing f from 0.008 to 0.014 with the step of 0.002, the change of ΔS is no less than five times the incident wavelength (2.9 μm). Our proposed structure is very sensitive to the chirality and the concentration of TDBCs and has potential applications in distinguishing the chirality detector.

Keywords: surface plasmon polaritons, chirality, Goos–Hanchen shift

PACS: 73.20.Mf **DOI:** 10.1088/1674-1056/abdda6

1. Introduction

During the past couple of years, the optical sensors at macro- and nano-scales have been investigated, and surface plasmon polaritons (SPPs) play an important role in these devices, such as sensors, detectors, even in quantum key distributions.[1–18] Goos–Hänchen (GH) shift is a small shift of light in the total internal reflection, which is quite sensitive to the surrounding medium.[1–10,12] Many applications are introduced in both theory and experiments, such as sensors,[3–5] resonance devices,[6] and switches based on Kretschmann configuration involving Kerr nonlinear medium.[7] Kretschmann configuration is a well-known configuration in SPP excitation.[7,12,19–22] GH shift can be directly measured in the experiment and can reach 100 times the incident wavelength.[7] If the medium in the Kretschmann configuration is chiral, GH would display a new function for detecting the chirality of the medium.

Chiral objects have many applications in bio-medicine and bio-agriculture.[23,24] Left-handed objects are beneficial to humans. Right-handed objects are harmful to pests and help to make a good harvest of the crops. Hence, it is very important to distinguish between left-handed and right-handed objects. During the recent works, SPPs and localized surface plasmons (LSPs) can enhance the electromagnetic fields in the near field and significantly amplify the chiral optical response.[25–42] Circular dichroism (CD) spectra are used to describe the chirality of the objects in a wide wavelength regime.[25–39] If we use the GH shift to replace the CD spectrum, the difference between the left molecules and the right molecules can be directly measured in the experiment, and we do not need to make a distinction of a small value between absorptions or scatterings.

In this paper, we investigate a chiral molecule detector based on the lateral shift splitting/GH shift splitting in Kretschmann configuration involving chiral tri (diethylene glycol monobutyl) citrates (TDBCs) by using classical methods. Kretschmann configuration is made up of a gold film sandwiched between the dielectric medium and left TDBCs or right TDBCs. Incident light is injected from the dielectric medium with an incident angle. Fresnel equations and the stationary phase method are employed to solve our proposed structure. The parameters of chiral TDBCs and Au film are changed to show the impact on the sensitivity of the molecule detector. Due to the direct measurement in the experiment,

*Project supported by Science and Technology Nova Plan of Beijing City, China (Grant No. Z201100006820122) and Fundamental Research Funds for the Central Universities, China.

†Corresponding author. E-mail: sg2010@bupt.edu.cn

© 2021 Chinese Physical Society and IOP Publishing Ltd

our structure has potential applications in distinguishing the chirality detector.

2. Calculation models and results

The sketch of our calculation model is shown in Fig. 1. An Au film with the thickness of d is sandwiched between the prism and chiral TDBCs. The incident chiral beam is injected from the dielectric medium with an incident angle θ. The dielectric constant function (ϵ_2) of Au is obtained in Ref. [43]. The index of the dielectric medium ($\sqrt{\epsilon_1}$) is chosen as $\sqrt{3.6}$. Chiral TDBCs are modeled by a Lorentzian oscillator[35,36]

$$\epsilon_3 = \epsilon_\infty + \frac{f_i \omega_i^2}{\omega_i^2 - \omega^2 - \mathrm{i}\gamma_i \omega}, \tag{1}$$

where i means left (L) or right (R), $\epsilon_\infty = n_{\mathrm{bg}}^2$, and $n_{\mathrm{bg}} = 1.33$ is the index of the background. ω_i is the resonant frequency of TDBCs, and γ_i is the damping constant of TDBC. f_i is the oscillator strength, which depends on the molecular concentration. According to the experimental measurement of TDBC, we obtain that $\omega_{\mathrm{L}} = 3.228 \times 10^{15}$ rad/s, $\omega_{\mathrm{R}} = 3.203 \times 10^{15}$ rad/s, and $\gamma_{\mathrm{L}} = \omega_{\mathrm{R}} = 8.195 \times 10^{13}$ rad/s.[35,36] Incident chiral beam is composed of TE-polarized beam ($\boldsymbol{E}_{\mathrm{s}}$) and TM-polarized beam ($\boldsymbol{E}_{\mathrm{p}}$) as $\boldsymbol{E}_{\mathrm{s}} + \boldsymbol{E}_{\mathrm{p}} \mathrm{e}^{\pm \mathrm{i}\pi/2}$. In Kretschmann configurations, only the TM-polarized beam can be used to generate SPPs. Here, we only consider TM-polarized beam is injected into our proposed system.

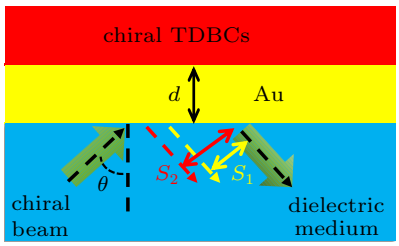


Fig. 1. The sketch of our calculation model.

GH shift S is calculated by the classical method as[2,7]

$$S = \frac{1}{\sqrt{\epsilon_1} k_0} \left| \frac{\mathrm{d}\phi_r}{\mathrm{d}\theta} \right|, \tag{2}$$

where $\phi_r = \mathrm{Im}(\ln r)$ is the phase of r, and r is TM-polarized reflection coefficients of Fresnel equations for Kretschmann configurations.[2,7,12] The reflection R is calculated as $R = |r|^2$. Before we discuss the relation between the GH shift S and the incident wavelength λ, it should be mentioned that the incident angle θ is equal to the surface plasmon resonant angle θ_{SPPs}.[2,7,44] In our calculation, the incident angle is changed with the incident wavelength. The best condition of SPP excitation is the angle being equal to the surface plasmon resonant angle θ_{SPPs}. In order to obtain a significant GH shift for each wavelength in calculations, we set the incident angle θ changing with the incident wavelength. In the application, we may set the incident angle θ is equal to θ_{SPPs} at the resonant wavelength of left TDBCs or right TDBCs. In the following, we calculate Kretschmann configurations with only LTDBCs and Right TDBCs to study normalized GH shift S/λ and the difference of normalized GH shifts between Kretschmann configurations with LTDBCs and RTDBCs $\Delta S/\lambda$.

3. Results and discussion

First, we choose $f_i = 0.01$ and $d = 20$ nm to calculate the reflection spectrum R and normalized GH shifts S/λ with both LTDBCs and RTDBCs, respectively. The incident angle is considered as θ_{SPPs}. The results are shown in Fig. 2. Furthermore, the difference of normalized GH shifts $\Delta S/\lambda$ is also plotted in Fig. 2.

Due to the interactions between SPPs and chiral TDBCs, normalized GH shifts S/λ are amplified near the resonant frequencies of chiral TDBCs, as shown in Fig. 2(a). They are as 24 times of LTDBCs and 10 times of RTDBCs as the incident wavelength. Due to the different resonant wavelengths, the positions of the maximum S for LTDBCs ($\lambda = 577$ nm) and RTDBCs ($\lambda = 582$ nm) do not overlap. As Fig. 2(b) shown, the difference of normalized GH shifts $\Delta S/\lambda$ can reach 24 at $\lambda = 577$ nm. It seems that the reflected beam with LTDBCs moves a lot, but the one with RTDBCs hardly moves at $\lambda = 577$ nm. This phenomenon can be easily measured in the experiment, and LTDBCs and RTDBCs are easily distinguished. Also, the working wavelength can be taken as $\lambda = 582$ nm.

Then, we decrease the thickness d of Au film to show how $\Delta S/\lambda$ changes. The thickness d is changed from 20 nm to 50 nm with the step of 10 nm. The results are shown in Fig. 3. For each thickness of the proposed system, S_i/λ is also calculated and shown in the inserted picture.

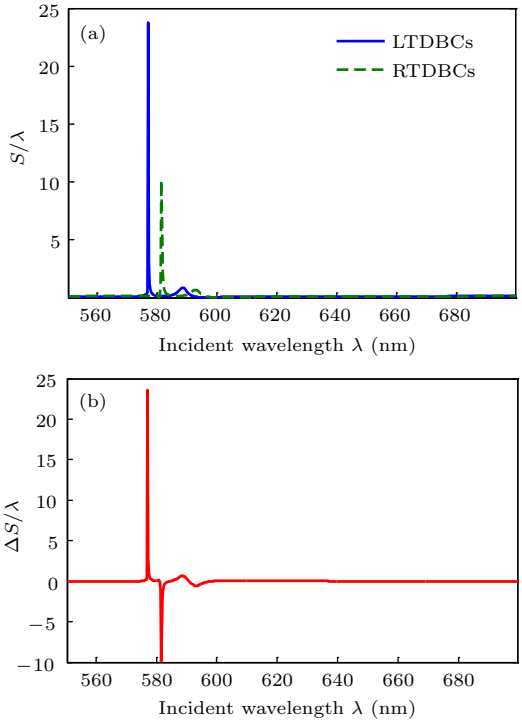


Fig. 2. Normalized GH shifts S_i/λ (a) and the difference of normalized GH shift $\Delta S/\lambda$ (b) versus the incident wavelength λ, respectively.

As shown in Fig. 3, the working wavelength of our proposed structure is changed by the thickness of Au film d. At the same time, the value of S_i/λ decreases. The dissipation of Au film increases sharply with the thickness of Au film increasing, while the decoupling conversion rate decreases. It means that there are more SPPs joining into the interaction between chiral TDBCs and Au film with the increase of Au film thickness. According to the analysis above, we can change the working wavelength by tuning the thickness of Au film. With the increase of d, the working wavelength has a red shift. Although there are more SPPs interact with chiral TDBCs, the intensity of $\Delta S/\lambda$ is reduced by the large dissipation. Comparing the intensity of $\Delta S/\lambda$, we also find that with the changes of d, there is an optimal thickness to make $\Delta S/\lambda$ the largest. We pick the maximum values and the positions of $\Delta S/\lambda$ for both LTDBCs and RTDBCs by changing d with the step of 0.5 nm. The results are shown in Fig. 4.

As shown in Fig. 4(a), there is a little difference between the optimal thicknesses for LTDBCs and RTDBCs. The largest $\Delta S/\lambda$ is larger than 100, which can be significantly observed in the experiments. The positions of the maximum of $\Delta S/\lambda$ for LTDBCs and RTDBCs almost do not overlap. The phenomena above are mainly caused by the different resonances for left TDBCs and right TDBCs. Besides the incident angle θ is equal to θ_{SPPs}, there is an optimal thickness of Au film which shows the best ability to coverts light into SPPs coupling with chiral TDBCs and decouple into light around the resonant wavelengths of chiral TDBCs. It reflects the competition between the dissipation and the conversion efficiency from light to SPPs. If the thickness of Ag film is less than the skin depth of light (less than 15 nm), light may directly go through Ag film without the electromagnetic field enhancement and couple with chiral TDBCs. This means that the chirality of TDBCs may not be amplified. According to our calculations, we'd better choose a suitable thickness of Au film to obtain obvious phenomenon for chiral TDBCs detecting in experiments.

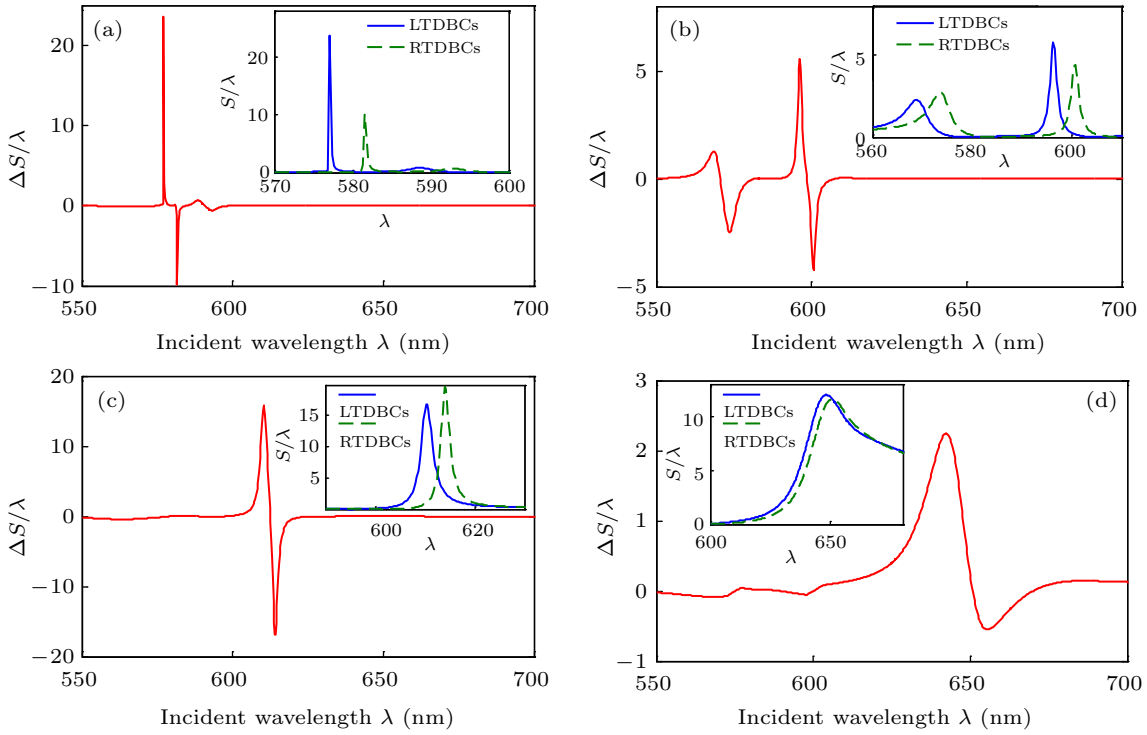


Fig. 3. The difference of normalized GH shift $\Delta S/\lambda$ versus the incident wavelength λ with Au film thickness d changing from 20 nm to 50 nm with the step of 10 nm, respectively. Normalized GH shifts S_i/λ versus the incident wavelength λ for each d is in the inserted picture.

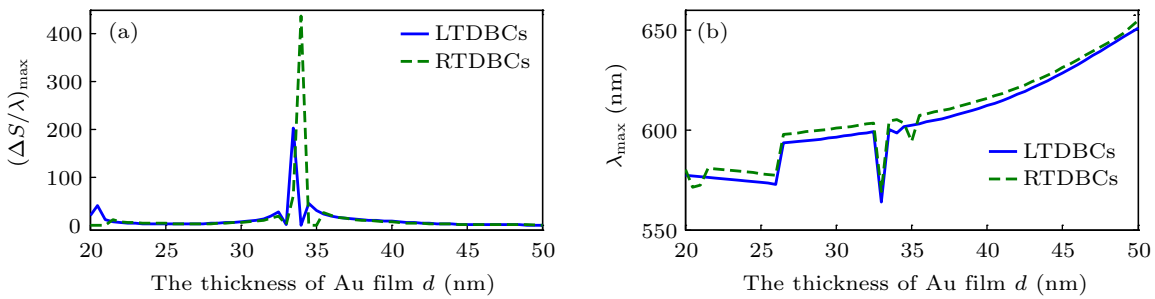


Fig. 4. The maximum values (a) and the positions (b) of $\Delta S/\lambda$ for both LTDBCs and RTDBCs by changing d with the step of 0.5 nm, respectively.

Table 1. The values of the peaks and dips in $\Delta S/\lambda$.

f	0.008	0.01	0.012	0.014
$\Delta S/\lambda(+)$	5.6 (579 nm)	23.6 (577 nm)	14.9 (576 nm)	6.9 (574 nm)
$\Delta S/\lambda(-)$	4.7 (584 nm)	9.8 (582 nm)	2.9 (580 nm)	8.0 (579 nm)

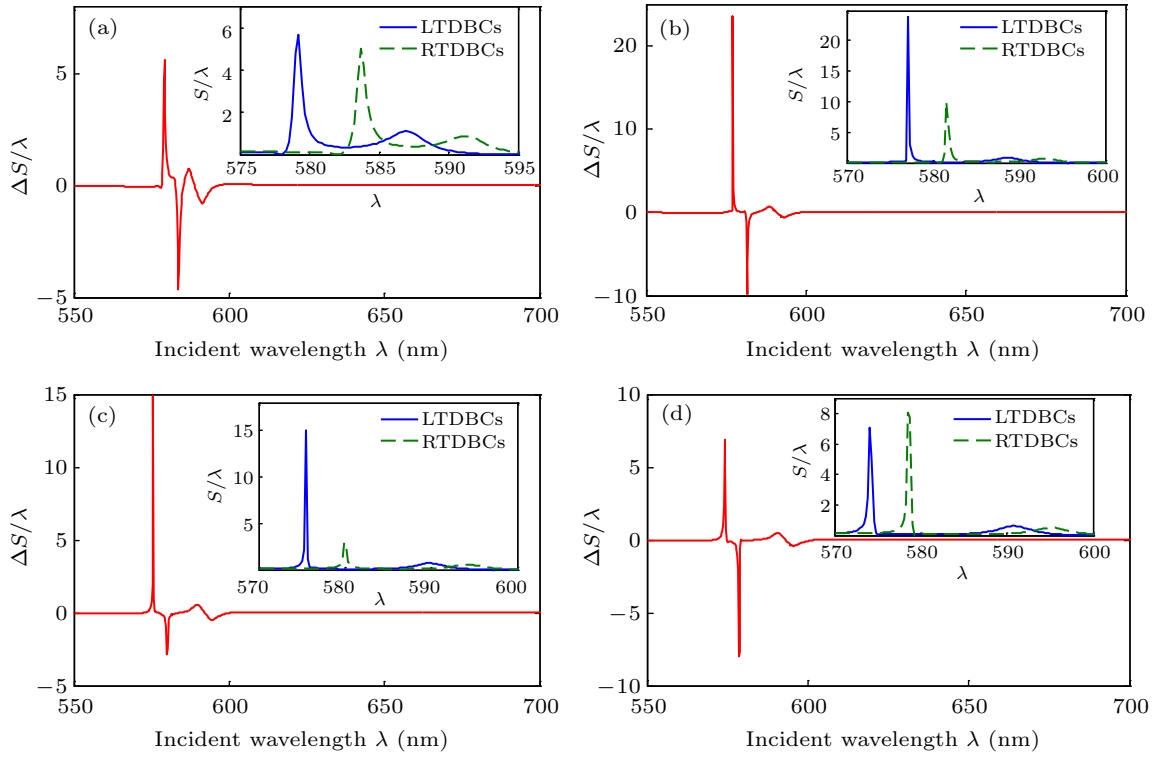


Fig. 5. The difference of normalized GH shift $\Delta S/\lambda$ versus the incident wavelength λ with coupling strength f changing from 0.008 to 0.014 with the step of 0.002, respectively. Normalized GH shifts S_i/λ versus the incident wavelength λ for each f is in the inserted picture.

Finally, we show the impact of the oscillator strength f on $\Delta S/\lambda$. We change a small step of 0.002 to show the sensitivity of our proposed structure. f is changed from 0.008 to 0.014, and $\Delta S/\lambda$ versus λ are shown in Fig. 5. S_i/λ is also inserted in the figures for each f.

As Fig. 5 shown, the peaks and the dips of $\Delta S/\lambda$ have a slight shift (within 5 nm) due to a quite small change of f. The values of the peaks and the dips in $\Delta S/\lambda$ changes a lot. This is because that f has great influences on ϵ_3 and θ_{SPPs}. Hence, the value of $\Delta S/\lambda$ changes a lot. We list the values of the peaks and the dips in Table 1. We find that although f changes a little 0.002, the difference of GH shifts between peak values or dip values is no less than 5 times of the incident wavelength, about 2.9 μm. This difference is easy to observe in the experiment.

4. Summary

In summary, we investigate a high sensitive chiral molecule detector based on GH shift in Kretschmann configuration involving chiral TDBCs. Fresnel equations and the stationary phase method are employed to calculate the lateral shift/GH shift. Due to the interaction between SPPs and the chiral TDBCs, the GH shifts in our proposed structures with two kinds of chiral TDBCs are amplified at different wavelengths. GH shift can reach 24 times the incident wavelength and be easily observed in the experiment. The working wavelength of the detector can be tuned by the thickness of the Au film. We also find there is an optimal thickness to make ΔS the largest, which is over 100 as the incident wavelength and can be easily observed in experiments. Furthermore, we discuss the oscillator strength f and find that our proposed detector is quite sensitive with f. By changing 0.002 for f, the change of ΔS is no less than 5 times the incident wavelength, which is about 2.9 μm at our working wavelength. Our proposed structure is very sensitive and has potential applications in experiments.

References

[1] Goos F and Hanchen H 1947 *Ann. der Phys.* **436** 333
[2] Artmann K 1948 *Ann. der Phys.* **2** 87
[3] Johansen K, StaLberg R, Lundstro M I and Liedberg B 2000 *Measurement Sci. and Techn.* **11** 1630
[4] Chen C W, Wei C, Lin L S, Liao Z H and Lin H P 2007 *Appl. Opt.* **46** 5347
[5] Nie S H, Wang X, Li J J, Clinite R and Cao J M 2009 *Appl. Phys. Lett.* **94** 166101
[6] Yin X B, Hesselink L, Liu Z W, Fang N and Xiang Z 2004 *Appl. Phys. Lett.* **85** 372
[7] Zhou H C, Chen X, Hou P and Li C F 2008 *Opt. Lett.* **33** 1249
[8] Fan Y H, Shen N H, Zhang F L, Wei Z Y, Li H Q, Zhao Q, Fu Q H, Zhang P, Koschny T and Soukoulis C M 2016 *Adv. Opt. Mater.* **4** 1824
[9] Kang J H, Wang S, Shi Z W, Zhao W Y, Yablonovitch E and Wang F 2017 *Nano Lett.* **17** 1768

[10] Alamri M, Zubairy M S and Zeng X D 2017 *Opt. Express* **25** 23579
[11] Lee J S, Huynh T, Lee S Y, Lee K G, Lee J Y, Tame M, Rockstuhl C and Lee C Y 2017 *Phys. Rev. A* **96** 033833
[12] Pang K W, Li H H, Song G and Zhang P F 2019 *Mod. Phys. Lett. B* **33** 1950370
[13] Liu Y, Cao F L, Liu J K, Xiao L and Shen Z K 2019 *Chin. Phys. B* **28** 028504
[14] Jiang Z, Sun Y Y, Guo C Y, Lv Y X, Hao H Y, Jiang D W, Wang G W, Xu Y Q and Niu Z C 2019 *Chin. Phys. B* **28** 038504
[15] Gao R L, Liu Y, Ouyang X P, Chen J and Ouyang X 2019 *Sci. China Phys. Mech. and Astron.* **62** 122012
[16] Liu L Y, Ouyang X, Ruan J L, Bai S and Ouyang X P 2019 *IEEE Trans. on Nuclear Science* **66** 737
[17] Fan Yuan G J, Wang S, Yin Z Q, Chen W, He D Y, Guo G C and Han Z F 2020 *Quantum Engineering* **2** e56
[18] Chai G, Li D W, Cao Z W, Zhang M H and Zeng G H 2020 *Quantum Engineering* **2** e37
[19] Bellessa J, Bonnand C, Plenet J C and Mugnier J 2004 *Phys. Rev. Lett.* **93** 036404
[20] Ouyang Q L, Zeng S W, Jiang L, Hong L Y, Xu G X, Dinh X Q, Qian J, He S L, Qu J L and Coquet P 2016 *Sci. Rep.* **6** 28190
[21] Moreau J, Bryche J F, Olivero A, Barbillon G, Coutrot A L, Bartenlian B, Sarkar M, Besbes M and Canva M 2015 *ACS Photon.* **2** 237
[22] Memmi H, Benson O, Sadofev S and Kalusniak S 2017 *Phys. Rev. Lett.* **118** 126802
[23] Hentschel M, Schäferling M, Duan X Y, Giessen H and Liu N 2017 *Sci. adv.* **3** e1602735
[24] Patterson D, Schnell M and Doyle J M 2013 *Nature* **497** 475
[25] George J and Thomas K G 2010 *J. Am. Chem. Soc.* **132** 2502
[26] Sun M T, Zhang Z L, Wang P J, Li Q, Ma F C and Xu H X 2013 *Light: Sci. & Applications* **2** e112
[27] Kuzyk A, Schreiber R, Fan Z Y, Pardatscher G, Roller M A, Högele A, Simmel F C, Govorov A O and Liedl T 2012 *Nature* **483** 311
[28] Maoz B M, Chaikin Y L, Tesler A B, Elli O B, Fan Z Y, Govorov A O and Markovich G 2013 *Nano Lett.* **13** 1203
[29] Zhang S P, Wei H, Bao K, Häkanson U, Halas N J, Nordlander P and Xu H X 2011 *Phys. Rev. Lett.* **107** 096801
[30] Govorov A O, Fan Z Y, Hernandez P, Slocik J M and Naik R R 2010 *Nano Lett.* **10** 1374
[31] Chervy T, Azzini S, Lorchat E, Wang S J, Gorodetski Y, Hutchison J A, Berciaud S, Ebbesen T W and Genet C 2018 *ACS Photon.* **5** 1281
[32] Alizadeh M H and Reinhard B M 2015 *ACS Photon.* **2** 1780
[33] Jiang Q B, Pham A, Berthel M, Huant S, Bellessa J, Genet C and Drezet A 2016 *ACS Photon.* **3** 1116
[34] Lan X and Wang Q B 2016 *Adv. Mater.* **28** 10499
[35] Song G, Guo J Q, Duan G Y, Jiao R Z and Yu L 2020 *Nanotechnology* **31** 345202
[36] He T T, Ye Q H and Song G 2020 *Chin. Phys. B* **29** 97306
[37] Ye F, Merlo J M, Burns M J and Naughton M J 2014 *Nanophoton.* **3** 33
[38] Liu Y, Ke Y G, Luo H L and Wen S C 2016 *Nanophoton.* **6** 51
[39] Afshinmanesh F, White J S, Cai W S and Brongersma M L 2012 *Nanophoton.* **1** 125
[40] Darweesh A, Bauman S, Debu S and Herzog J 2018 *Nanomaterials* **8** 809
[41] Wang Y D, Liu H X, Wang S L, Cai M, Zhang H F and Qiao Y B 2020 *Nanomaterials* **10** 2012
[42] Vyshnevyy A A and Fedyanin D Y 2020 *Nanomaterials* **10** 856
[43] Palik E D 1998 *Handbook of optical constants of solids* (Vol. 3) (Academic Press)
[44] Maier S A 2007 *Plasmonics: Fundamentals and Applications* (Springer Press)